The Free Internet Journal
for Organic Chemistry

Paper

Archive for
Organic Chemistry

Arkivoc **2026**, part __, 0-0
to be inserted by editorial office

Facile synthesis of symmetrical di([1,1′-biphenyl]-4-yl) phthalates *via* Pd catalyzed Suzuki-Miyaura coupling with comparative vibrational and rotational analysis using DFT

Muhammad Zubair[a], Adeel Mubarik[b], Abid Mahmood[c], Maria Sohail[a], Nasir Rasool[a*], Aqsa Kanwal[a], Gulraiz Ahmad[a]

[a] *Department of Chemistry, Government College University Faisalabad, Faisalabad, 38000, Pakistan.*
[b] *School of Chemistry and Chemical Engineering, Nanjing University of Science and Technology, Nanjing 210094, People's Republic of China*
[c] *Department of Pharmaceutical Chemistry, Government College University Faisalabad, Faisalabad 38000, Pakistan*
Email: nasirrasool@gcuf.edu.pk

Received mm-dd-yyyy **Accepted** mm-dd-yyyy **Published on line** mm-dd-yyyy

Dates to be inserted by editorial office

Abstract

In this study, the successful synthesis of bis(4-bromophenyl) phthalates through the reaction of phthaloyl chloride with 4-bromophenol and di([1,1'-biphenyl]-4-yl) phthalates *via* a Suzuki-Miyaura coupling is described. DFT analyses were performed to deepen our understanding of the spectroscopic and thermodynamic characteristics of synthesized compounds. Thermodynamic features, such as HOMO and LUMO as frontier molecular orbitals, MESP, and IP, EA, χ, ω, η, μ, and S (reactivity descriptors) were studied in PBE0-D3BJ/def2-TZVP theory level for structure elucidation of the synthesized derivatives.

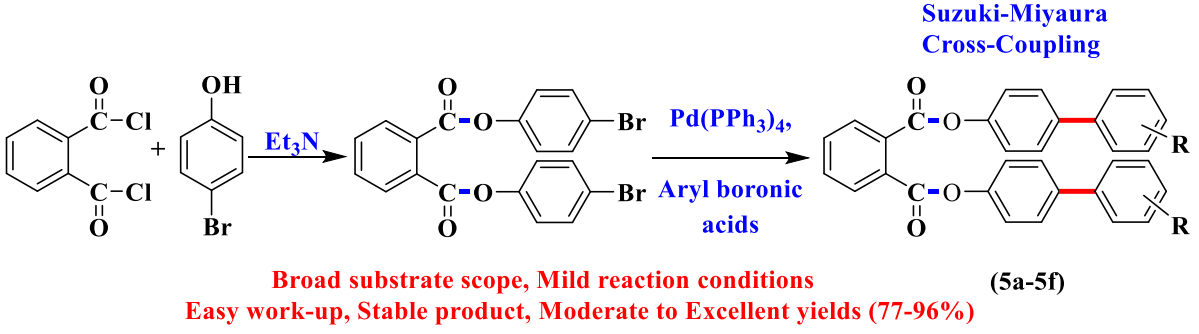

Keywords: Phthalic acid esters , di([1,1'-biphenyl]-4-yl) phthalates, Suzuki-Miyaura cross-coupling, density functional theory, comparative spectral studies; potential energy distribution.

Introduction

PAEs (Phthalic acid esters), generally known as phthalates, are a lipophilic class of chemicals extensively used as additives and plasticizers in plastics to enhance plasticity, durability, flexibility, UV degradation resistance and combustion.[1] PAEs are widely utilized in approximately each manufacturing and are generally found in construction constituents, varnish, latex paint, printing inks, cosmetics and personal care products, clothing, food packaging, medical products, intravenous cannulas, pharmaceutics, and insecticides. Some of the most extensively used PAEs include BBP (butyl benzyl phthalate), DBP (dibutyl phthalate), DEHP (di(2-ethylhexyl) phthalate), DINP (di-isononyl phthalate), and DIDP (di-isodecyl phthalate).[2] Yeon Bang *et al.* reported the synthesis of polymer electrolytes comprising of NaI and I_2 dissolved in PEO (poly(ethylene oxide) and DOP (dioctyl phthalate) as an additive and applied the synthesized electrolytes to DSSC (dye-sensitized solar cells) displayed 2.9% of overall ECE (energy conversion efficiency).[3] Phthalate plasticizers are the most commonly employed category among all plasticizer types because of their excellent plasticizing properties and price advantages.[4] Chen *et al.* compared comprehensive efficiencies for antistatic and transparent plasticized PVC (polyvinyl chloride) films with diverse plasticizers (DINP, DPHP (dipropyl heptyl phthalate), PPA (poly(propylene adipate)).[5]

Based on the reports mentioned, researchers have increasingly favored the development of plasticizers that possess conductivity and other comprehensive performances. Inspired by various research analyses on phthalate derivatives present in the literature mainly as electrolytes in optoelectronic device fabrication and various other purposes, Thus, we were prompted to examine evaluating the vibrational (IR, PED%) through DFT of bis(4-bromophenyl) phthalate (**3**) through Schotten-Baumann reaction [6, 7] and their di([1,1'-biphenyl]-4-yl) phthalates (**5a–5f**) analogs through Suzuki-Miyaura coupling reactions.[8]

To validate the wavenumber assignments of synthesized derivatives (**5a-5f**), DFT functional computations have also been executed.[9] Moreover, the calculated spectra in terms of PED have been interpreted and according to PED study, each vibrational mode has been assigned.[10-12] PBE0-D3BJ/def2-TZVP theory level functional has previously exhibited an excellent conciliation between computational efficiency and accuracy of vibration spectra for large/medium-sized compounds.[13-15] It is often observed that the frequencies of vibration calculated through computational quantum chemistry are frequently greater than experimentally determined alternates, hence empirical scaling parameters are commonly applied to improve the experimental vibrational patterns.[16] These scaling factors are determined by mean deviation towards the predicted and experimentally determined frequencies, which depends on the computational method and basis sets used to perform computations.[17-20] For this purpose, we used DFT studies to compute the geometrical properties and vibrational frequency spectrum of tailored bis(4-bromophenyl) phthalates in the ground state. We also measured the estimated values of vibrating experimentally determined frequencies. This will provide new insight into the molecular parameters and vibrational spectrum for further studies in the future.

In the present research work, we reported synthesis and comparison of arylated phthalates' theoretical and experimental spectral results (**5a–5f**). To current knowledge, no extensive quantum chemical computations or vibrational spectra of di([1,1'-biphenyl]-4-yl) phthalate analogs have been described previously. So, the current research aims to thoroughly investigate the vibrational spectra and identify the modes with increased wavenumber precision.

 ©AUTHOR(S)

Results and Discussion

Bis(4-bromophenyl) phthalate (**3**) was synthesized by the reaction of phthaloyl chloride (**1**) and 4-bromophenol (**2**) in the presence of Et_3N as a base and CH_2Cl_2 to obtain the desired product up to 98% at room temperature. Later, the Suzuki-Miyaura–coupling of bis(4-bromophenyl) phthalate (**3**) with several aryl boronic acids (**5a-5f**) in the presence of the $Pd(PPh_3)_4$ (tetrakis(triphenylphosphine)palladium(0)) and K_3PO_4 as a mild base yielded targeted compounds (**5a–5f**) in fair to good yields (77–96%) (Scheme 1, Figure 1). The reaction optimization given below indicated that the K_3PO_4 and 1,4-dioxane/toluene are the best base and solvent respectively (**Table 1**). It was observed that the electron-rich ring activating group gives a good yield but the electron-rich boronic acid with two substitutions gives an excellent product yield (**5a**). However, it was also experimentally observed that the electron-poor substituted boronic acids give a very low yield of a product as in **5f,** due to electron-withdrawing substitution of chloro group at *meta* and fluoro at *para* position leads to ring deactivation. Notably, it was also observed that increasing catalyst loading gives a higher yield. However, it was also observed that a moderately strong base as potassium phosphate (K_3PO_4) gives an excellent yield, than cesium carbonate (Cs_2CO_3) that hydrolyzed the Suzuki-Miyaura coupled product ultimately leads to lower yield. Here, the effect of the solvent was never negligible. Furthermore, mild base sodium carbonate (Na_2CO_3) gives a very low yield. Surprisingly, in Suzuki-Miyaura coupling, stable products were formed through optimized conditions. The synthesized compounds (**5a-5f**) were purified from flash column chromatography. They were characterized by various spectroscopic techniques (^{1}HNMR and ^{13}CNMR), and elemental analysis. The low yield may be associated with challenging purification by column chromatography.[21]

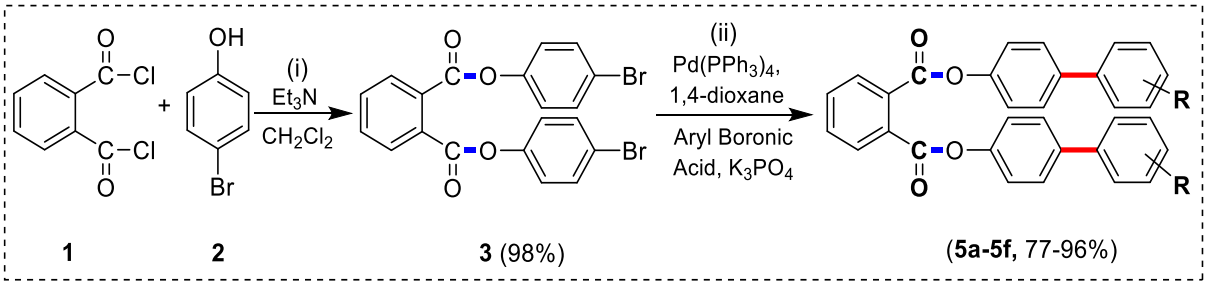

Scheme 1. Synthesis of bis(4-bromophenyl) phthalate (**3**) and di([1,1'-biphenyl]-4-yl) phthalates (**5a–5f**). **Reagents and conditions:** (i) **1** (0.92 mL, 1.0 eq. 6.40 mmol, **2** (2.32 g, 2.1 eq. 13.44 mmol), Et_3N (2.23 mL, 2.5 eq.), in DCM (15 mL), stirred for 2 h at room temperature. (ii) **3** (0.20 g, 0.42 mmol, 1 eq), $Pd(PPh_3)_4$ (0.03 g, 7 mol%), K_3PO_4 (0.35g, 1.68 mmol, 4.0 eq.), aryl boronic acids (1.1 eq., 0.46 mmol), 1, 4-dioxane/toluene (10 mL) (1:1), H_2O (1mL), reflux at 85-90 °C, 24 h.

©**AUTHOR(S)**

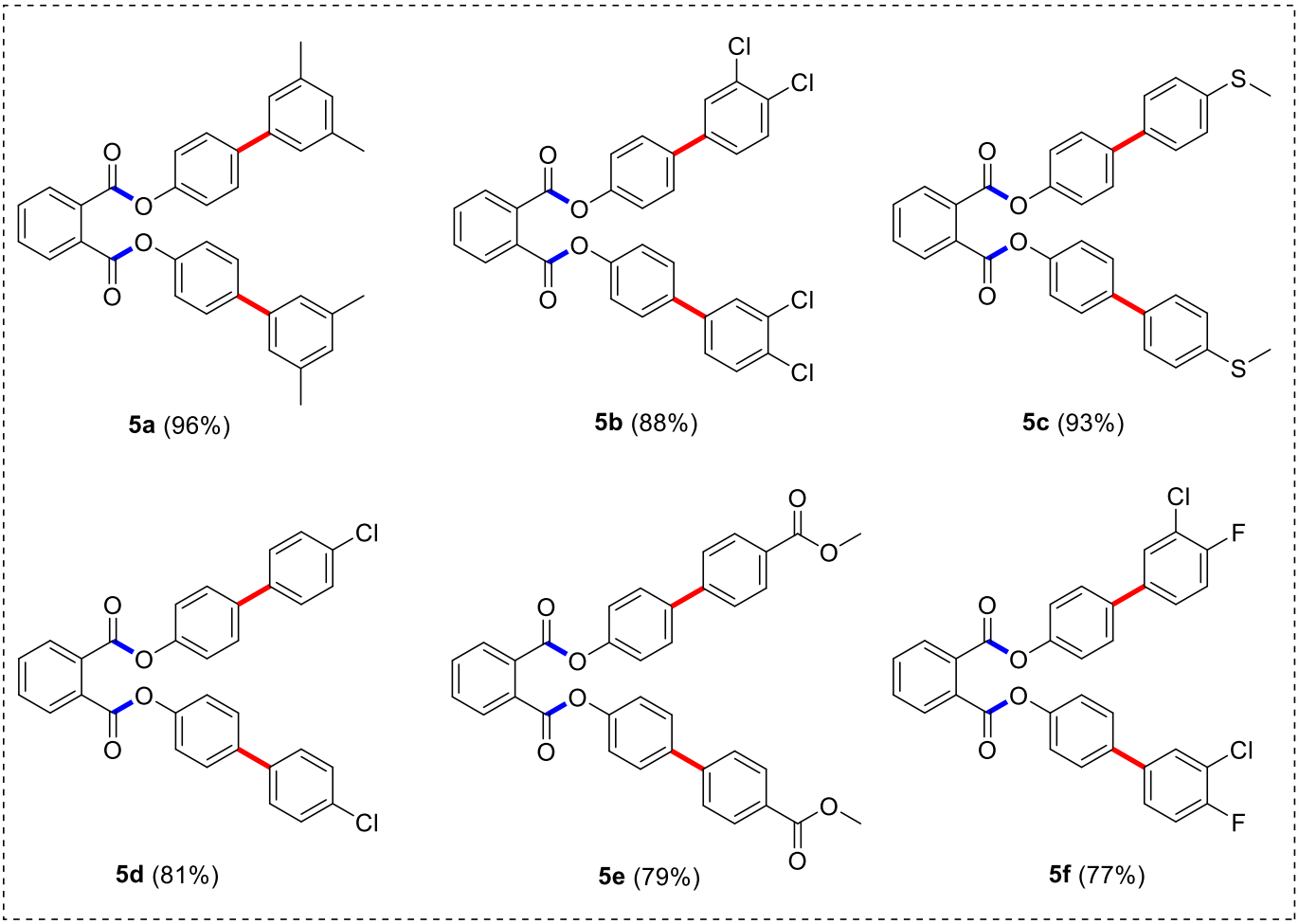

Figure 1. An overview of the structures of the di([1,1'-biphenyl]-4-yl) phthalates **(5a–5f)** and their percentage yields.

Table 1. Optimization of catalyst, solvents, and base for Suzuki-Miyaura coupling (**5a**).

Entry	Base	Catalyst loading	Solvents	Yield
1	Na_2CO_3	2.5 mol%	Toluene	51
2	Na_2CO_3	5 mol%	Toluene	54
3	Cs_2CO_3	2.5 mol%	Toluene	57
4	Cs_2CO_3	5 mol%	1,4-dioxane/toluene	72
5	K_3PO_4	5 mol%	1,4-dioxane/toluene	93
6	**K_3PO_4**	**7 mol%**	**1,4-dioxane/toluene**	**96**

©AUTHOR(S)

Computational details

All calculations in the current research work were performed through DFT with the PBE0-D3BJ/def2-TZVP theory level[22] as implemented in the Gaussian 09 program.[23, 24] This basis set was chosen due to its reasonable balance between accuracy and computational cost for the system under investigation. Initially, the ground-state optimized geometries of the synthesized di([1,1'-biphenyl]-4-yl) phthalates (**5a–5f**) were calculated to ensure that the geometries correspond to stable configurations of the compounds (Figure 2). The optimized electronic structures obtained in this study relate to energy minima, as evidenced by the absence of imaginary frequencies in the vibrational frequency analysis. The electronic properties of the molecule by calculating the HOMO and the LUMO energies to examine the electronic structure and the molecule stability. The Molecular Electrostatic Potential (MEP) is also investigated to visualize the electron density distribution across the molecule's surface. Key reactivity descriptors such as IP, EA, χ, η, and μ were also determined to understand the molecule's chemical reactivity and polarity. Chemical potential was calculated providing further insight into the compound's stability. The spectroscopic features such as vibrational and nuclear magnetic resonance (NMR) spectra were also measured to compare with the experimental data. PED analysis, carried out with VEDA 4 program[25] facilitated the assignment of vibrational modes, supporting the understanding of molecular vibrations.[26, 27] The ^{1}H NMR spectroscopic shifts (δ) of synthesized derivatives (**5a-5f**), were calculated from GIAO (gauge-independent atomic orbit) approach, where theoretically measured shifts were in good agreement with experimentally determined values**.** The combined use of computational and experimental methods in this study highlights the importance of DFT calculations in predicting molecular behavior and guiding future research in organic synthesis.

3.2 NMR rotational Spectroscopy

NMR spectroscopy is the most significant method for accurately identifying the structural framework of organic molecules. Theoretically determined Quantum calculations have been proven to be suitably precise in computing NMR spectra and examining the link towards chemical shifts and its molecular structure.[28, 29] Thus, applying theoretical approaches may strengthen confidence in describing structure of synthesized derivatives.[30] NMR spectroscopic calculations were done for all simulated molecules at same theoretically determined level as optimization and then compared with experimental NMR data. In Table 2, experimentally and theoretically calculated ^{1}H NMR spectroscopy data of synthesized derivative **5a** have been explained for comparison while the remaining compounds (**5b-5f**), ^{1}H NMR spectroscopy data are given in Supplementary data (Tables S2–S6). Mean absolute deviation can be expressed as mean absolute error, while root-mean-square deviation as root-mean-square error. Boltzmann-averaged values are given in respective tables which strongly correlate with experimentally determined data. It can be observed that the performance of NMR spectroscopy calculations of **5a** is very good and MAE (mean absolute error) is only 0.43 ppm (Table 2).

Table 2. Comparison of experimentally determined and theoretically calculated ^{1}H NMR data of synthesized derivative **5a**.

 ©AUTHOR(S)

Carbon No.	Carbon Type	^{1}H-NMR (δ, ppm) Experimentally determined	^{1}H-NMR (δ, ppm) Computed theoretically	Δδ, ppm
1	CH	8.04	7.45	0.59
2	CH	7.73	7.19	0.54
3	CH	7.67	7.21	0.46
4	CH	7.94	6.98	0.96
8	CH	7.51	6.83	0.68
9	CH	7.58	7.10	0.48
11	CH	7.58	7.18	0.40
12	CH	7.51	7.00	0.51
14	CH	7.27	6.90	0.37
16	CH	6.99	6.56	0.43
18	CH	7.27	6.78	0.49
19	CH_3	2.38	2.17	0.21
20	CH_3	2.38	2.23	0.15
8'	CH	7.11	6.93	0.18
9'	CH	7.58	7.05	0.53
11'	CH	7.58	6.93	0.65
12'	CH	7.11	6.60	0.51
14′	CH	7.27	6.65	0.62
16′	CH	6.99	6.51	0.48
18′	CH	7.27	6.68	0.59
19′	CH_3	2.38	2.11	0.27
20′	CH_3	2.38	2.05	0.33

MAE (Mean Absolute Error) = **0.43**

RMSE (Root Mean Square Error) = **0.48**

©AUTHOR(S)

Comparative IR and PED of compound 5a

The vibrational frequencies of the synthesized compound were experimentally measured and compared with computationally calculated frequencies (both unscaled and scaled) and potential energy distribution (PED) values.[31] This validation process was crucial for assigning each vibrational frequency based on potential energy distribution (PED), allowing for a clearer interpretation of the molecular vibrations.[32] The comparison reveals strong agreement between experimental and calculated frequencies, with notable vibrations observed at C-H stretching 3013 cm^{-1}, 2916 cm^{-1}, 2851 cm^{-1} (C-H stretching), 1735 cm^{-1} (-O-C=O ester stretching), 1684 cm^{-1} (C=O carbonyl stretch), C-C stretching and bending 1597 cm^{-1}, 1507 cm^{-1}. The PED analysis, which assigns specific vibrational modes, shows significant contributions for C-H stretching, C-C stretching, and bending modes, with higher PED values corresponding to dominant vibrations such as the C-H stretches (97%) and C=O stretches (89%) (Table 3). Noteworthy, the correlation between experimental and computational vibrational frequencies confirms the reliability of the theoretical model. Higher stability, indicated by a larger HOMO-LUMO energy gap (ΔE), corresponds to higher vibrational frequencies due to stronger bonding interactions. Conversely, smaller ΔE values suggest increased electron delocalization, leading to weaker bonds and lower vibrational modes. Since vibrational modes are influenced by electronic distribution, particularly molecular orbitals, the HOMO-LUMO gap analysis was conducted to explore further the electronic properties, mainly charge transfer, reactivity, and stability of synthesized compounds (**5a-5f**).

Table 3. Experimental and calculated Frequencies with PED% and vibrations of Compound **5a**.

Experimental Frequencies (cm^{-1})	Calculated Frequencies		PED %	Vibrations
	Unscaled value (cm^{-1})	Scaled value (cm^{-1})		
3013	3266	3005	97	*s* (CH)
2916	3163	2910	64	*s* (CH)
2851	3053	2808	30	*s* (CH)
1735	1890	1739	89	*s* (COO)
1684	1866	1716	89	*s* (CO)
1597	1687	1552	29	*s* (CC)
1507	1684	1549	24	*s* (CC)
-	1660	1527	29	*s* (CC)
1479	1567	1442	19	*b* (HCC)
1395	1512	1391	12	*s* (CC)
1259.	1363	1254	13	*s* (CC)
-	1360	1252	14	*s* (CC)
1190	1292	1189	37	*s* (CO)
1161	1266	1164	20	*s* (CO)
1127	1239	1140	11	*s* (CC)

 ©AUTHOR(S)

1038	1129	1038	30	*b* (HCC)
-	1127	1036	31	*b* (HCC)
877	930	855	16	*t* (HCCC)
849	921	847	22	*t* (HCCC)
803	879	809	11	*b* (CCC)
726	796	733	16	*O* (OCOC)
-	752	692	10	*t* (CCCC)

s=Stretching, *t*=Torsional, *b*=Bending, *O*= out of plane bending

FMO analysis

HOMO and LUMO, energy gaps collectively named frontier orbitals, are employed to study various electronic features, reactivity, and tendency towards stability of molecules.[14, 20, 24] The energy gap (ΔE) serves as a key indicator of stability, with smaller gaps correlating with higher reactivity and greater potential for electron transfer, while larger gaps indicate increased stability and reduced reactivity. The larger the ΔE more stability and less reactivity of the compound while the opposite is true when ΔE is smaller. The less ΔE shows the ultimate intramolecular charge interaction is high. Arylated phthalates with diverse functional groups have a strong potential to modify the sites and ΔE of HOMO-LUMO orbitals (Figure 3). This change in ΔE gaps impacts charge transitions that occur in various reactivity features. As therefore, the reactivity features of any compound structure may be altered through inserting alternative functional substitutions onto their structural cores, ultimately changing their ΔE **(**energy gaps). DFT calculations at the PBE0-D3BJ/def2-TZVP level were performed to analyze the HOMO-LUMO energy gap, which was found to range from 4.16 eV (**5c**) to 4.87 eV (**5e**). In the series **5a–5f**, **5c** exhibits the lowest energy gap of 4.16 eV, indicating its least stability and highest reactivity due to thiomethyl substitution at a para position leads to electron delocalization and enhances charge transfer ability by increasing π-electron delocalization. In contrast, **5e** displays the highest ΔE **(**energy gap) of 4.87 eV, suggesting its highest stability and least reactivity. However, the theoretically calculated $E_{LUMO,}$ E_{HOMO}, E_{HOMO}-E_{LUMO} gap (ΔE) values of di([1,1'-biphenyl]-4-yl) phthalate (**5a-5f**) are enlisted in Table 4, and Figure 3.

 ©AUTHOR(S)

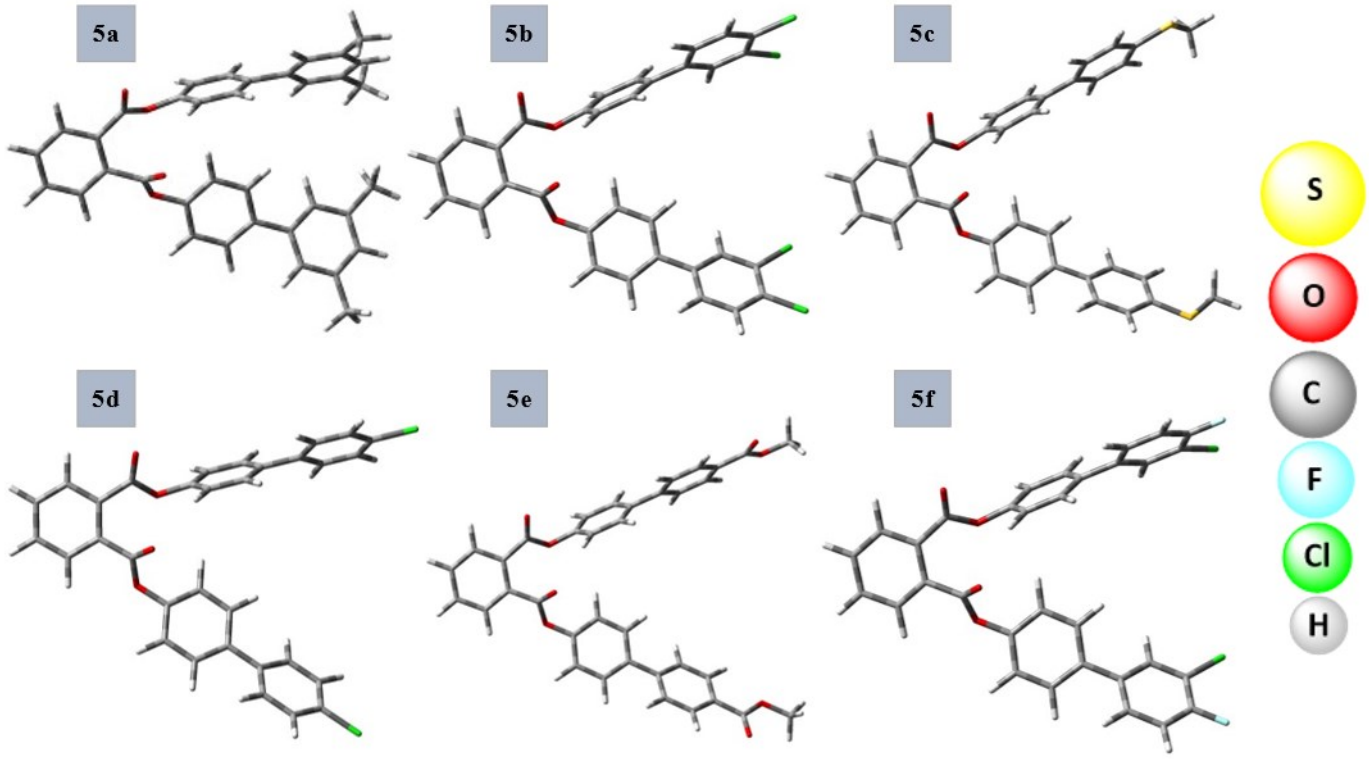

Figure 2. 3D Optimized structures of synthesized derivatives (**5a–5f**) by the PBE0-D3BJ/def2-TZVP theory level

Table 4. Theoretically calculated values of E_{LUMO}, E_{HOMO}, E_{HOMO}-E_{LUMO} gap (ΔE) of synthesized derivatives (**5a–5f**).

Compounds	E_{HOMO}	E_{LUMO}	ΔE
5a	-6.30	-1.65	4.65
5b	-6.57	-1.77	4.81
5c	-5.79	-1.63	4.16
5d	-6.47	-1.71	4.76
5e	-6.64	-1.77	4.87
5f	-6.56	-1.74	4.82

©**AUTHOR(S)**

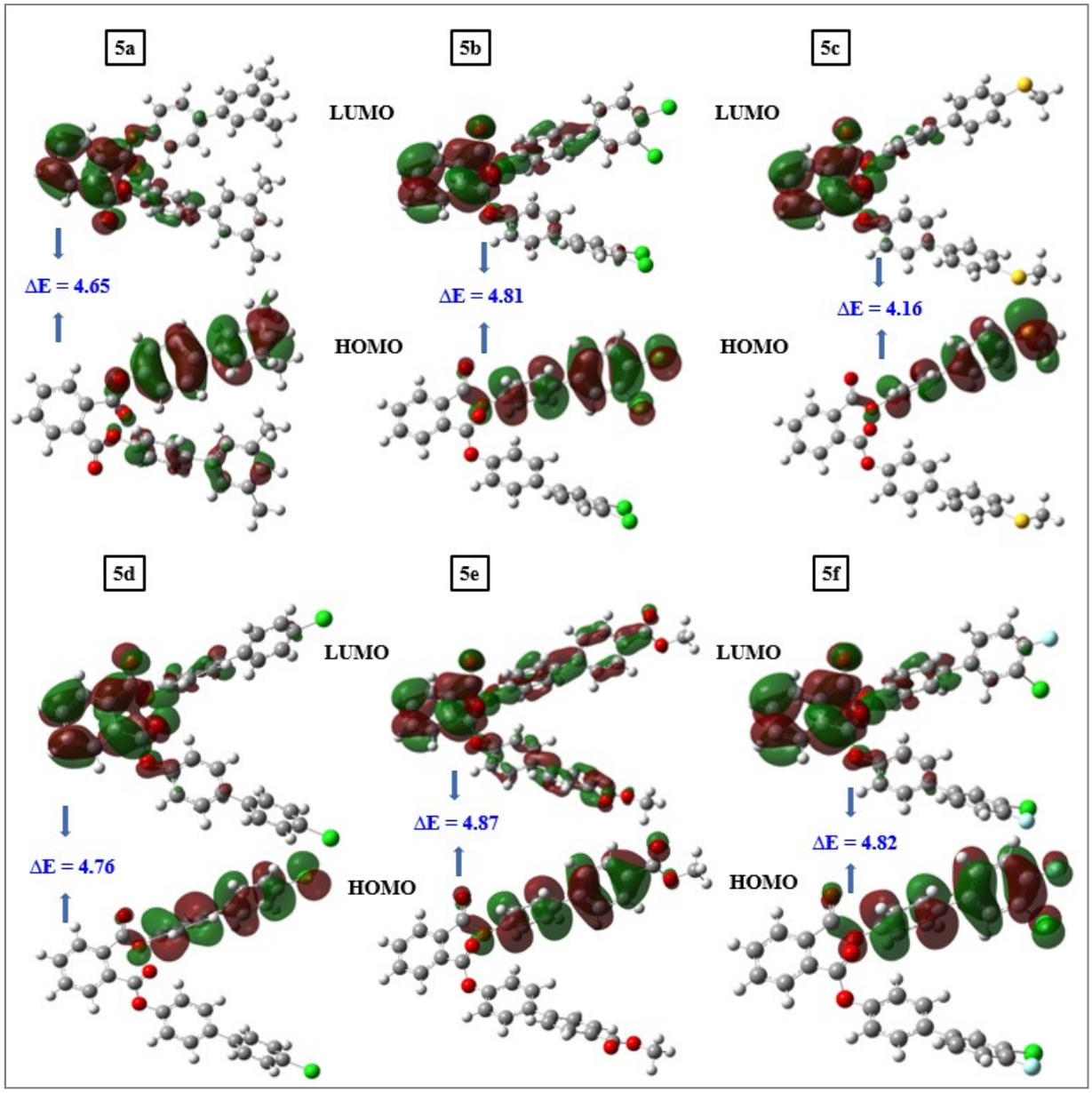

Figure 3. Molecular Orbitals (HOMO-LUMO) of arylated analogs of bis(4-bromophenyl) phthalates (**5a–5f**) calculated at PBE0-D3BJ/def2-TZVP level of theory.

Molecular electrostatic potential analysis (MESP)

©**AUTHOR(S)**

MEP is highly valuable in analyzing molecular structure and its physiochemical parameter associations.[33, 34] The MEP illustrates the electrostatic potential distribution, molecular structure, size, and dipole moments of the molecule, and it provides a visual tool for understanding relative polarity. The molecular electrostatic potential can be used to calculate the reactive sites of molecules. Figure 4 depicts the MEP of each chemical. The color scheme for the MEP surface for partially negative charge or electron-rich is red color, for electron-deficient or partially positive charge is blue color, light blue for slightly electron deficient zone, and yellow for slightly electron-rich region. The MEP clearly shows negative regions (red colored) that are focused around the compound's heteroatoms (nitrogen, oxygen, sulfur, and halogens). These sites are favorable for an electrophilic attack. The blue colored (positive regions) indicates the possible sites for a nucleophilic attack are localized around the aromatic benzene rings. MEP surfaces indicate the feasible sites readily available for the electrophilic and nucleophilic reaction pathways.

Figure 4. Molecular electrostatic potentials maps of (**5a–5f**)

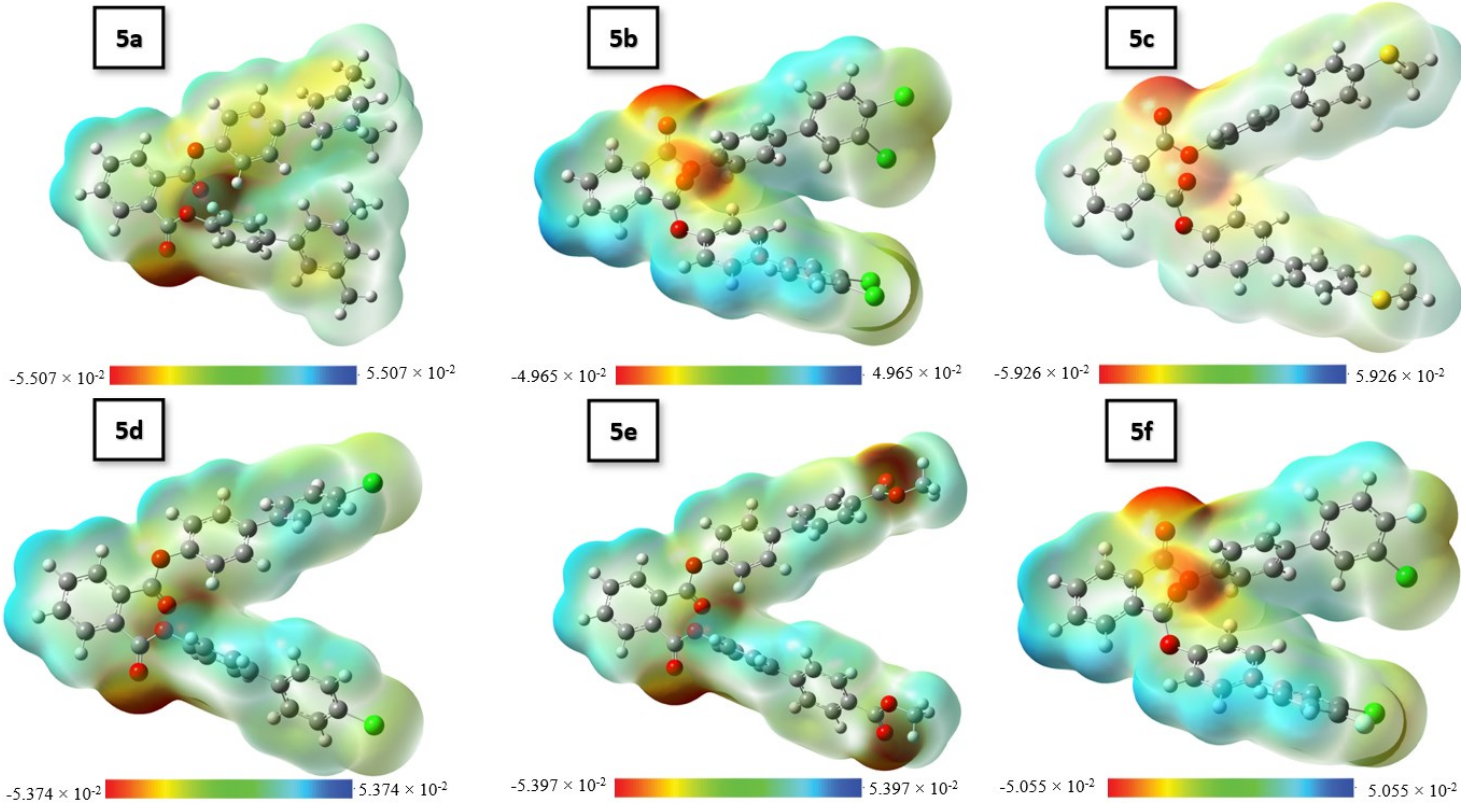

Reactivity descriptors

Although electrons have a key part in several chemical reactions, HOMO and LUMO have an impact on a molecule's chemical reactivity patterns. **ΔE** energy gap can be employed to determine structural stability. Generally, in synthesized derivatives (**5a-5f**), a larger energy gap is quite more stable than compounds with a smaller ΔE gap. A smaller ΔE energy gap indicates that charge transfer is easy within orbitals, leading the compound to be soft and reactive, whereas a big energy gap needs more energy for transitions, making the molecule structure rigid and hence not as reactive. The Ionization energies and electron affinities are calculated via Koopman's theorem.[18] Softness (S) is the inverse of hardness (η) and reflects the extent of reactivity, IP (Ionization potential) was calculated as $-E_{HOMO}$, and EA (electron affinity) as $-E_{LUMO}$. In contrast, electronegativity (χ), electrophilicity index (ω), chemical hardness (η), chemical potential (μ), and global

 ©**AUTHOR(S)**

softness (S) were determined using Eq. 1–5, which have been reported in many research studies [19, 35, 36] and are reported in Table 5.

$$\chi = [IP+EA]/2 = -[E_{LUMO}+E_{HOMO}]/2 \quad (1)$$

$$\eta = [IP-EA]/2 = -[E_{LUMO}-E_{HOMO}]/2 \quad (2)$$

$$\mu = [E_{LUMO}+E_{HOMO}]/2 \quad (3)$$

$$S = 1/\eta \quad (4)$$

$$\omega = \mu^2/2\eta \quad (5)$$

Table 5 The reactivity descriptors of all synthesized derivatives (**5a–5f**)

Compound	Electron Affinity (EA)	Ionization Potential (IP)	Electro-negativity (χ)	Electro philicity (ω)	Chemical Potential (μ)	Global Hardness (η)	Global Softness (S)
5a	1.65	6.30	3.97	3.39	-3.97	2.33	0.43
5b	1.77	6.58	4.17	3.62	-4.17	2.40	0.41
5c	1.63	5.79	3.71	3.32	-3.71	2.08	0.48
5d	1.71	6.47	4.09	3.51	-4.09	2.38	0.42
5e	1.77	6.64	4.21	3.64	-4.21	2.43	0.41
5f	1.74	6.57	4.15	3.58	-4.15	2.41	0.41

Conclusions

Bis(4-bromophenyl) phthalate (**3**) was synthesized by treating with Phthaloyl chloride and 4-bromophenol, following synthesis of arylated phthalates (**5a–5f**) *via* SMC. The structural characterization of the synthesized compounds was comprehensively performed using a combination of experimental spectroscopic techniques, including nuclear magnetic resonance (NMR) and infrared (IR) spectroscopy, and supported by density functional theory (DFT) calculations. These approaches allowed us to confirm the identity and structure of the compounds, with the NMR chemical shifts and IR vibrational modes showing excellent agreement with experimental results. Thermodynamic and chemical parameters, such as HOMO and LUMO energy differences, were also calculated by computation to assess the stability and reactivity of the compounds. Most and least reactive compounds in the series (**5a–5f**) are identified by comparing energies to the entire compounds. **5c** exhibits the lowest ΔE of 4.16 eV, indicating its least stability in the synthesized series (**5a-5f**). In contrast, **5e** displays the highest ΔE gap of 4.87 eV, suggesting its highest stability. These calculations not only provided insights into the compounds' electronic properties but also highlighted the reactivity trends within the series. The molecular electrostatic potential maps identify active sites for electrophilic and nucleophilic attacks. The analysis of spectroscopic features, including vibrational (IR, PED%) and NMR spectroscopy, was performed and correlated with experimental data. Utilizing the VEDA 4 program for PED analysis allowed for the effective assignment of vibrational modes. The ^{1}H NMR spectroscopy shifts (δ) were calculated using the GIAO technique, yielding results that are consistent with experimental findings.

 ©**AUTHOR(S)**

Integrating computational and experimental methods comprehensively studies the molecules' synthesis, reactivity, and structural properties, increasing their potential utility in diverse domains.

Experimental Section

General. FT-IR spectrum of synthesized compounds was found in the 4000-650 cm^{-1} ranges. Through KBr disc protocol, the FT-IR were recorded at 300 K at solid phase. Samples' infrared spectra were measured using a 1000 FT-IR Mattson spectrometer. Melting points of freshly synthesized derivatives (5a-5f) were calculated with B-540 (Buchi) equipment. Macklin China provided chemicals used in present study. The spectroscopic study employed the Advance III Bruker spectrometer to investigate the NMR spectra of yielded molecules in deuterated $CDCl_3$. The *J* (coupling constant) has been taken in Hz, whereas *δ* (chemical shift) was determined in ppm. To purify the synthesized derivatives (5a-5f), column chromatography with silica gel having mesh size 200-400 was employed. LECO CH micro analyzer (630–200-200 TruSpec) was utilized for elemental analysis.

Synthesis of bis(4-bromophenyl) phthalate (**3**). Phthaloyl chloride (0.92 mL, 6.4 mmol, 1.0 eq.) was mixed with 4-bromophenol (2.32 g, 13.4 mmol, 2.1 eq.), after which 2.23 mL of triethylamine was added dropwise at 0°C to the mixture. Then the reaction mixture was stirred in the presence of dichloromethane (DCM) as a solvent (15 mL) at room temperature for 2 h. The final product was obtained as pink crystals after workup by adding H_2O to the reaction mixture. The reaction mixture and water were extracted three times with 30 mL DCM.[8, 21] The lower layer was separated and dried with a rotary evaporator under reduced pressure. The target compound was characterized using NMR spectroscopy.

Synthesis of di([1,1'-biphenyl]-4-yl) phthalates (**5a–5f**). The calculated amount of bis (4-phenylphthalate) (0.20 g), palladium catalyst in the form of tetrakis (triphenylphosphine) (0.03 g) and 1, 4-dioxane/toluene (10 mL) having a ratio (1:1) was taken in the Schlenk tube that was washed and then dried in an oven. The reaction was stirred for 30 min at room temperature in an inert atmosphere by using argon gas. 2.2 eq. of aryl boronic acid and 4.0 eq. of K_3PO_4 were added and then 1 mL of distilled water was added to reaction mixture *via* using a syringe and then kept on stirring until the reaction mixture was completed at 85-90°C. The reaction was continuously monitored through TLC chromatography after every 3-4 h. The mixture was then filtered with the help of ethyl acetate and then purified through column chromatography with a ratio of ethyl acetate/*n*-hexane (1:9). The purified product was then analyzed *via* ^{1}H-NMR and ^{13}C-NMR spectroscopy.[21, 37-40]

Bis(4-bromophenyl) phthalate (**3**). Yield 98 %; Light pink crystals; M.P. 194°C. ^{1}H NMR (400 MHz, $CDCl_3$) δ 7.96 (dd, J = 5.7, 3.3 Hz, 2H), 7.68 (dt, J = 7.3, 3.6 Hz, 2H), 7.52 – 7.48 (m, 4H), 7.10 (dd, J = 9.4, 2.6 Hz, 4H). ^{13}C NMR (101 MHz, $CDCl_3$) δ 165.5, 149.7, 132.6, 132.1, 131.3, 129.6, 123.3, 119.4. Elemental Anal. Calcd. for $C_{20}H_{12}Br_2O_4$ (476.12): C, 50.45; H, 2.54% Found: C, 50.41; H, 2.57%.

Bis(3',5'-dimethyl-[1,1'-biphenyl]-4-yl) phthalate (5a). Yield 96%; White crystals; M.P. 224-225 °C. ^{1}H NMR (400 MHz, $CDCl_3$) δ 8.04 – 7.94 (m, 2H), 7.73 – 7.67 (m, 2H), 7.58 (d, 4H), 7.51 (dd, *J* = 8.8, 2.1 Hz, 2H), 7.30 – 7.24 (m, 4H), 7.11 (dd, 2H), 6.99 (s, 2H), 2.38 (s, 12H). ^{13}C NMR (101 MHz, $CDCl_3$) δ 166.0, 150.0, 140.3, 139.5, 138.3, 132.6, 131.9, 129.7, 129.0, 128.3, 125.1, 123.4, 123.3, 121.7, 21.4. Elemental Anal. Calcd. for $C_{36}H_{30}O_4$ (526.63): C, 82.11; H, 5.73% Found: C, 82.09; H, 5.67%.

Bis(3',4'-dichloro-[1,1'-biphenyl]-4-yl) phthalate (5b). Yield 88%; Brown solids; M.P. 224-226 °C. ^{1}H NMR (400 MHz, $CDCl_3$) δ 8.01 (dd, *J* = 5.7, 3.3 Hz, 2H), 7.76 – 7.66 (m, 2H), 7.63 (d, *J* = 2.2 Hz, 2H), 7.54 (d, *J* = 2.0 Hz, 4H), 7.48 (d, *J* = 8.3 Hz, 2H), 7.37 (dd, *J* = 8.4, 2.2 Hz, 2H), 7.31 (d, 4H). ^{13}C NMR (101 MHz,

 ©**AUTHOR(S)**

$CDCl_3$) δ 165.8, 150.7, 140.2, 136.8, 132.9, 132.0, 131.6, 131.5, 130.7, 129.6, 128.9, 128.2, 126.3, 122.1. Elemental Anal. Calcd. for $C_{32}H_{18}Cl_4O_4$ (608.29): C, 63.19; H, 2.98% Found: C, 63.14; H, 2.91%.

Bis(4'-(methylthio)-[1,1'-biphenyl]-4-yl) phthalate (5c). Yield 93%; Light yellow crystals; M.P. 218-219°C. ^{1}H NMR (400 MHz, $CDCl_3$) δ 8.03 – 7.94 (m, 2H), 7.70 (d, *J* = 3.1 Hz, 2H), 7.57 (d, *J* = 2.1 Hz, 4H), 7.48 – 7.36 (m, 4H), 7.33 – 7.27 (m, 4H), 7.12 (d, *J* = 8.8 Hz, 4H), 2.51 (s, 6H). ^{13}C NMR (101 MHz, $CDCl_3$) δ 165.8, 155.3, 150.0, 138.7, 132.6, 131.9, 129.7, 128.0, 127.4, 127.1, 126.9, 123.4, 122.0, 15.8. Elemental Anal. Calcd. for $C_{34}H_{26}O_4S_2$ (562.70): C, 72.57; H, 4.66% Found: C, 72.49; H, 4.65%.

Bis(4'-chloro-[1,1'-biphenyl]-4-yl) phthalate (5d). Yield 81%; White crystals; M.P. 214-217 °C. ^{1}H NMR (400 MHz, $CDCl_3$) δ 7.99 (d, 2H), 7.70 (d, 2H), 7.54 (d, 4H), 7.47 – 7.41 (m, 4H), 7.40 – 7.36 (m, 4H), 7.29 (dd, *J* = 11.6, 8.5 Hz, 4H). ^{13}C NMR (101 MHz, $CDCl_3$) δ 169.7, 155.3, 139.2, 132.7, 129.0, 128.8, 128.3, 128.2, 128.1, 127.9, 122.0, 115.7. Elemental Anal. Calcd. for $C_{32}H_{20}Cl_2O_4$ (539.41): C, 71.25; H, 3.74% Found: C, 71.26; H, 3.76%.

Bis(4'-(methoxycarbonyl)-[1,1'-biphenyl]-4-yl) phthalate (5e). Yield 79%; Brown crystals; M.P. 223-2243 °C. ^{1}H NMR (400 MHz, $CDCl_3$) δ 8.01 (dd, *J* = 6.1, 3.0 Hz, 2H), 7.96 – 7.89 (m, 2H), 7.73 – 7.68 (m, 4H), 7.50 (d, 4H), 7.31 (d, *J* = 8.3 Hz, 4H), 7.13 (d, *J* = 8.7 Hz, 4H), 3.93 (s, 6H). ^{13}C NMR (101 MHz, $CDCl_3$) δ 166.8, 165.5, 149.7, 144.3, 132.6, 132.0, 131.3, 130.2, 129.6, 127.2, 123.3, 119.4, 52.2. Elemental Anal. Calcd. for $C_{36}H_{26}O_8$ (586.60): C, 73.71; H, 4.47% Found: C, 73.68; H, 4.45%.

Bis(3'-chloro-4'-fluoro-[1,1'-biphenyl]-4-yl) phthalate (5f). Yield 77%; Grey crystals; M.P. 211-213 °C. ^{1}H NMR (400 MHz, $CDCl_3$) δ 8.13 – 8.10 (m, 2H), 7.96 (dd, *J* = 5.7, 3.3 Hz, 2H), 7.70 (d, *J* = 3.2 Hz, 2H), 7.69 (d, *J* = 1.6 Hz, 2H), 7.68 – 7.65 (m, 2H), 7.50 (d, 4H), 7.09 (d, 4H). ^{13}C NMR (101 MHz, $CDCl_3$) δ 167.75, 165.48, 149.65, 144.33, 132.62, 132.00, 131.31, 130.19, 129.56, 127.23, 123.30. Elemental Anal. Calcd. for $C_{32}H_{18}Cl_2F_2O_4$ (575.39): C, 66.80; H, 3.15% Found: C, 66.75; H, 3.17%.

Acknowledgements

The authors gratefully acknowledge the PCSIR (Ministry of Science and Technology), to access sophisticated equipment through the data repository of the scientific instrumentation development program initiated in 2021.

Supplementary Material

Supplementary data associated with this article are available in the Electronic Supplementary Material (ESI).

References

Al-Harethi, 1. Kumar, R.; Verma, A.; Shome, A.; Sinha, R.; Sinha, S.; Jha, P. K.; Kumar, R.; Kumar, P.; Shubham; Das, S. *Sustainability* **2021**, 13, 1-40. https://doi.org/10.3390/su13179963.

2. Huang, L.; Zhu, X.; Zhou, S.; Cheng, Z.; Shi, K.; Zhang, C.; Shao, H. *Toxins* **2021**, 13, 495. https://doi.org/410.3390/toxins13070495.

 ©**AUTHOR(S)**

3. Bang, S. Y.; Lee, K. J.; Koh, J. H.; Kang, M.-S.; Kang, Y. S.; Kim, J. H. *Ionics* **2008**, 14, 143-148. https://doi.org/110.1007/s11581-11007-10173-11580.
4. Dong, X.; Long, M.; Liu, H.; Gao, L.; Xu, X.; Xia, X. *Appl. Polym. Sci.* **2023**, 140, e53905. https://doi.org/53910.51002/app.53905.
5. Chen, M.; Yang, B.; Zhang, J. *Appl. Polym. Sci.* **2024**, 141, e56021. https://doi.org/56010.51002/app.56021.
6. Arranz, F.; Chaves, M. S.; Gil, F. *Angew. Makromol. Chem.* **1980**, 92, 121-132. https://doi.org/110.1002/apmc.1980.050920110.
7. Gümüş, M.; Babacan, Ş. N.; Demir, Y.; Sert, Y.; Koca, I.; Gülçin, İ. *Arch. Pharm.* **2022**, 355, 2100242. https://doi.org/2100210.2101002/ardp.202100242.
8. Siddiqa, A.; Zubair, M.; Bilal, M.; Rasool, N.; Qamar, M. U.; Khalid, A.; Ahmad, G.; Imran, M.; Mahmood, S.; Ashraf, G. A. *Pharmaceuticals* **2022**, 15, 1-14. https://doi.org/10.3390/ph15070841.
9. Lokhande, S. R.; Adole, V. A.; Rajesh, R.; Mali, S. N.; Sadgir, N. V.; Islam, M. S.; Almutairi, T. M.; Cruz, J. N.; Patil, M. P.; Jagdale, B. S. *J. Mol. Struct.* **2025**, 141761. https://doi.org/141710.141016/j.molstruc.142025.141761.
10. Güllüoğlu, M.; Erdogdu, Y.; Karpagam, J.; Sundaraganesan, N.; Yurdakul, Ş. *J. Mol. Struct.* **2011**, 990, 14-20. https://doi.org/10.1016/j.molstruc.2011.1001.1001.
11. Mariappan, G.; Sundaraganesan, N. *J. Mol. Struct.* **2014**, 1063, 192-202. https://doi.org/110.1016/j.molstruc.2014.1001.1064.
12. Elkaeed, E. B.; Mughal, E. U.; Kausar, S.; Al-ghulikah, H. A.; Naeem, N.; Altaf, A. A.; Sadiq, A. *J. Mol. Struct.* **2022**, 1270, 1-14. https://doi.org/10.1016/j.molstruc.2022.133972.
13. Maqbool, T.; Younas, H.; Bilal, M.; Rasool, N.; Bajaber, M. A.; Mubarik, A.; Parveen, B.; Ahmad, G.; Ali Shah, S. A. *ACS Omega* **2023**, 8, 30306-30314. https://doi.org/30310.31021/acsomega.30303c03183.
14. Balakit, A. A.; Makki, S. Q.; Sert, Y.; Ucun, F.; Alshammari, M. B.; Thordarson, P.; El-Hiti, G. A. *Supramol. Chem.* **2020**, 32, 519-526. https://doi.org/510.1080/10610278.10612020.11808217.
15. Shinde, R. A.; Adole, V. A.; More, R. A.; Jagdale, B. S.; Waghchaure, R. H.; Gurav, S. S.; Mali, S. N. *J. Mol. Struct.* **2025**, 1322, 140313. https://doi.org/140310.141016/j.molstruc.142024.140313.
16. Ojha, J. K.; Ramesh, G.; Reddy, B. V. *Chem. Phys. Impact.* **2023**, 7, 1-8. https://doi.org/10.1016/j.chphi.2023.100280.
17. Basha, F.; Khan, F. L. A.; Muthu, S.; Raja, M. *Comput. Theor. Chem.* **2021**, 1198, 113169. https://doi.org/113110.111016/j.comptc.112021.113169.
18. Schrader, T.; Khanifaev, J.; Perlt, E. *Chem Commun.* **2023**, 59, 13839-13842. https://doi.org/13810.11039/D13833CC04304E.
19. Suresh, C. H.; Remya, G. S.; Anjalikrishna, P. K. *Wiley Interdiscip. Rev. Comput. Mol. Sci.* **2022**, 12, 1-31. https://doi.org/10.1002/wcms.1601.
20. Abdulridha, A. A.; Allah, M. A. A. H.; Makki, S. Q.; Sert, Y.; Salman, H. E.; Balakit, A. A. *J. Mol. Liq.* **2020**, 315, 113690. https://doi.org/113610.111016/j.molliq.112020.113690.
21. Hafeez, J.; Sabir, A.; Rasool, N.; Hafeez, U.; Siddique, F.; Bilal, M.; Kanwal, A.; Ahmad, G.; Alqahtani, F.; Imran, I. *Arab. J. Chem.* **2024**, 17, 1-18. https://doi.org/10.1016/j.arabjc.2024.105889.
22. Fakhar M.; Zaman, U.; Mubarik, A.; Kanwal, A.; Rasool, N.; Ahmad, M.; Sohail, M.; Malik, A.; Al-Hussain, S. A.; Zaki, M. E. *Catalysts* **2025**, 15, 713. https://doi.org/710.3390/catal15080713.
23. Sieffert, N.; Wipff, G. *Dalton Trans.* **2015**, 44, 2623-2638. https://doi.org/2610.1039/C2624DT02443E.
24. Gökce, H.; Şen, F.; Sert, Y.; Abdel-Wahab, B. F.; Kariuki, B. M.; El-Hiti, G. A. *Molecules* **2022**, 27, 2193. https://doi.org/2110.3390/molecules27072193.

 ©AUTHOR(S)

25. Jamróz, M. H. *Spectrochim. Acta, Part A* **2013**, 114, 220-230. https://doi.org/210.1016/j.saa.2013.1005.1096.
26. Benbouguerra, K.; Chafai, N.; Chafaa, S.; Touahria, Y. I.; Tlidjane, H. *J. Mol. Struct.* **2021**, 1239, 1-11. https://doi.org/10.1016/j.molstruc.2021.130480.
27. Dege, N.; Gökce, H.; Doğan, O. E.; Alpaslan, G.; Ağar, T.; Muthu, S.; Sert, Y. *Colloids Surf., A* **2022**, 638, 128311. https://doi.org/128310.121016/j.colsurfa.122022.128311.
28. Bühl, M.; van Mourik, T. *Wiley Interdiscip. Rev.:Comput. Mol. Sci.* **2011**, 1, 634-647. https://doi.org/610.1002/wcms.1063.
29. Marcarino, M. O.; Zanardi, M. a. M.; Cicetti, S.; Sarotti, A. M. *Acc. Chem. Res.* **2020**, 53, 1922-1932. https://doi.org/1910.1021/acs.accounts.1920c00365.
30. Krivdin, L. B. *Molecules* **2021**, 26, 1-65. https://doi.org/10.3390/molecules26092450.
31. Sert, Y.; Çırak, Ç.; Ucun, F. *Spectrochim. Acta, Part A* **2013**, 107, 248-255. https://doi.org/210.1016/j.saa.2013.1001.1046.
32. Bozuyla, M.; Bayrakdar, A.; Sert, Y.; Kart, H. H.; Kart, S. O.; Manivannan, P.; Alma, M. H. *J. Comput. Chem.* **2025**, 46, e70098. https://doi.org/70010.71002/jcc.70098.
33. Saidj, M.; Djafri, A.; Rahmani, R.; Belkafouf, N. E. H.; Boukabcha, N.; Djafri, A.; Chouaih, A. *Polycyclic Aromat. Compd.* **2023**, 43, 2152-2176. https://doi.org/2110.1080/10406638.10402022.12039238.
34. Kocakaya, Z.; Sert, Y.; Kocakaya, M.; Karatoprak, G. Ş.; İlgün, S.; Çadır, M. *J. Mol. Struct.* **2025**, 417, 126660. https://doi.org/126610.121016/j.molliq.122024.126660.
35. Chermette, H. *J. Comput. Chem.* **1999**, 20, 129-154. https://doi.org/110.1002/(SICI)1096-1987X(19990115)19990120:19990111%19990113C19990129::AID-JCC19990113%19990113E19990113.19990110.CO;19990112-A.
36. Sable, Y. R.; Adole, V. A.; Pithawala, E. A.; Amrutkar, R. D. *J. Sulphur Chem.* **2025**, 1-26. https://doi.org/10.1080/17415993.17412025.12461582.
37. Tùng, Đ. T.; Tuân, Đ. T.; Rasool, N.; Villinger, A.; Reinke, H.; Fischer, C.; Langer, P. *Adv. Synth. Catal.* **2009**, 351, 1595-1609. https://doi.org/1510.1002/adsc.200900044.
38. Khalid, S.; Sabir, A.; Mohsin, N.; Rasool, N.; Imran, I.; Siddique, F.; Nadeem, S.; Kanwal, A.; Alqahtani, F.; Imran, M. *ChemistrySelect* **2025**, 10, e03224. https://doi.org/03210.01002/slct.202503224.
39. Sharif, M.; Mahmood, A.; Kanwal, A.; Ahmad, M.; Rasool, N.; Qamar, M. U.; Mughram, M. H. A.; A. A. M.; Shah, T. A.; Shaikh, I. I. *Sci. Rep.* **2025**, 15, 25661. https://doi.org/25610.21038/s41598-25025-10048-25664.
40. Abbas, M.; Sohail, M.; Rasool, N.; Qamar, M. U.; Mahmood, A.; Kanwal, A.; Mubarik, A.; Hassan, S.; Imran, M.; Shah, A. A. *Chem. Afr.* **2025**, 8, 1-16. https://doi.org/10.1007/s42250-42025-01483-x.

This paper is an open access article distributed under the terms of the Creative Commons Attribution (CC BY) license (http://creativecommons.org/licenses/by/4.0/)